Analysis of Ginzburg-Landau-type models of surfactant-assisted liquid phase separation

Gyula I. Tóth*
Institute of Physics and Technology, University of Bergen, Allégaten 55, N-5007 Bergen, Norway
and Institute for Solid State Physics and Optics, Wigner Research Centre for Physics, P.O. Box 49, H-1525 Budapest, Hungary

Bjørn Kvamme
Institute of Physics and Technology, University of Bergen, Allégaten 55, N-5007 Bergen, Norway
(Received 20 November 2014; published 9 March 2015)

In this paper diffuse interface models of surfactant-assisted liquid-liquid phase separation are addressed. We start from the generalized version of the Ginzburg-Landau free-energy-functional-based model of van der Sman and van der Graaf. First, we analyze the model in the constant surfactant approximation and show the presence of a critical point at which the interfacial tension vanishes. Then we determine the adsorption isotherms and investigate the validity range of previous results. As a key point of the work, we propose a new model of the van der Sman/van der Graaf type designed for avoiding both unwanted unphysical effects and numerical difficulties present in previous models. In order to make the model suitable for describing real systems, we determine the interfacial tension analytically more precisely and analyze it over the entire accessible surfactant load range. Emerging formulas are then validated by calculating the interfacial tension from the numerical solution of the Euler-Lagrange equations. Time-dependent simulations are also performed to illustrate the slowdown of the phase separation near the critical point and to prove that the dynamics of the phase separation is driven by the interfacial tension.

DOI: 10.1103/PhysRevE.91.032404 PACS number(s): 68.05.−n, 82.70.Uv, 68.03.Cd, 64.70.Ja

I. INTRODUCTION

Adding surfactants, i.e., interface active agents, to binary systems consisting of two immiscible fluids may effectively reduce the interfacial tension, thus leading to the formation of emulsions [1]. Emulsions play an important role in everyday life [2], ranging from medical issues [3,4] and pharmaceutical materials [5], through cosmetics and food processing [6], to crude oil recovery [7,8]. The latter has continuously increasing industrial importance: It has been discovered that alternating water and CO_2 injection is a significantly more efficient enhanced oil recovery technique than injecting exclusively water or CO_2 [9,10], predicting the water/CO_2 emulsion to be an effective material for oil recovery. Some of the possible emulsifiers are promising candidates to form water/hydrocarbon emulsions as well, thus further increasing the recovery rate significantly. This concept would also be economically more advantageous than conventional aquifer CO_2 sequestration.

The dynamics of emulsion formation is governed by the microscopic properties of the surfactant-loaded liquid-liquid interface, which can be addressed by atomistic simulations. Molecular dynamics simulations provide data on the interfacial properties of the two-phase system on the microscopic level. These data can be then used as input for continuum descriptions addressing mesoscale phenomena. Diffuse interface theories are one branch of continuum theories working with space and time continuous *order parameter* fields. Some of them are based on the Ginzburg-Landau theory of first-order phase transitions. Such descriptions originate from Gompper and Zschocke [11] and Theissen and Gompper [12]. The latter address fluid-flow-assisted spontaneous emulsification of the oil/water system, while the model of Teramoto and Yonezawa [13] has been successfully used to describe droplet growth dynamics in the same system. Despite their success, these relatively simple phenomenological approaches lack realistic Langmuir and Frumkin adsorption isotherms, therefore, a new, more realistic formulation was necessary. The most widespread version of Ginzburg-Landau-based surfactant models was published by van der Sman and van der Graaf [14], based on the regularization of the surface Dirac δ function of the sharp interface model of Diamant and Andelman [15]. The theory captures the essential effects of surfactants, in particular, the lowering of the interfacial tension with increasing surfactant load, and provides promising preliminary results for surfactant-laden droplet dynamics in sheared flow. A similar approach was published by Teng, Chern, and Lai [16]. Liu and Zhang [17] introduced a generalized model by extending the van der Sman/van der Graaf model with additional free energy terms accounting for lateral interaction between adjacent surfactant layers, as well as asymmetry in bulk fluids. The new model has been successfully applied to describe the influence of a nontrivial phenomenon, the Marangoni effect generated by the inhomogeneous interfacial tension on droplet dynamics. A comparative study of the aforementioned models was published by Li and Kim [18]. Despite their efforts, the models still suffered from some unphysical properties, such as decreasing interface width with increasing surfactant load. To avoid the problem, Yun, Li, and Kim [19] introduced a nonvariatinal formalism of the dynamic equations, however, the surfactant-free solution is no longer present in the new model. Nevertheless, they have also successfully addressed the Marangoni effect on droplet dynamics. A different method of fixing interface-related problems has been proposed by

*gyula.toth@ift.uib.no

Engblom and coworkers [20]. Besides the unphysical behavior of the interface width, the authors gave strong evidence that the partial differential equation (PDE) problem has no solution in physically relevant circumstances. In order to handle this problem, different surfactant couplings were proposed and analyzed, revealing that the decreasing tendency of the interface width can be reversed together with termination of the instability of the PDE system. This important finding opened the possibility of developing physically consistent diffuse interface models: When, in a two-phase liquid/surfactant system, the interfacial tension tends to 0 at a finite surfactant load, the phase separation critically slows down, thus a mechanically stable emulsion can form. This phenomenon has not yet been addressed as a function of the surfactant load and necessitates a detailed analysis of the interfacial tension. Finally, we mention that other, nonvariational, non-Ginzburg-Landau-based descriptions have also been developed, such as the one by Teigen and coworkers [21] addressing droplet breakup and coalescence.

The paper is structured as follows. In Sec. II we introduce a generalized van der Sman/van der Graaf–type free energy functional with the corresponding equilibrium (Euler-Lagrange) and dynamic equations. In Sec. III we analyze the equilibrium solutions: first, using the constant surfactant field approximation, we present simple analytical calculations for the interfacial tension, interface width, and speed of phase separation in the different variants of the model and show how the critical point (i.e., a critical surfactant load at which the interfacial tension vanishes) enters the model. Considering the result we propose a new version of the model in which the surfactant load dependence of the interface width cancels, establishing numerical efficiency. Next, we investigate the existence of the pure (surfactant-free) solution and calculate the adsorption isotherms, then carry out more precise analytical calculations to estimate the interfacial tension as a function of the surfactant load and analyze the behavior of the model at small surfactant loads and also near the critical point. In the first part of Sec. IV we briefly discuss the numerical methods used in solving the Euler-Lagrange equations and the dynamic equations. This is followed by numerical validation of the analytical formula for the interfacial tension. We also perform time-dependent simulations and verify the location of the critical point, together with analyzing the surfactant load dependence of the phase separation speed. In Sec. V we summarize the results.

II. THE MODEL

A. Free energy functional

Following van der Sman and van der Graaf the free energy of an inhomogeneous binary fluid + surfactant system is written as [14]

$$F = \int dV\{\mathcal{F}[\phi(\mathbf{r},t),\psi(\mathbf{r},t)]\}, \tag{1}$$

where $\phi(\mathbf{r},t)$ is the liquid-liquid order parameter and $\psi(\mathbf{r},t)$ the *volume fraction* of the surfactant. The integrand reads

$$\mathcal{F} = \mathcal{F}_{\mathrm{CH}} + \mathcal{F}_{\psi} + \mathcal{F}_{1} + \mathcal{F}_{\mathrm{ex}},$$

where

$$\mathcal{F}_{\mathrm{CH}} = w\, g(\phi) + \frac{\kappa}{2}(\nabla\phi)^2,$$

$$\mathcal{F}_{\psi} = \frac{w}{\beta}[\psi\log\psi + (1-\psi)\log(1-\psi)] - w\frac{c}{2}\psi^2,$$

$$\mathcal{F}_{1} = -\psi\left[\lambda_1\, w\, g(\phi) + \lambda_2\frac{\kappa}{2}(\nabla\phi)^2\right],$$

$$\mathcal{F}_{\mathrm{ex}} = w\left(\frac{a}{2}\phi^2 - e\phi\right)\psi.$$

Here $\mathcal{F}_{\mathrm{CH}}$ is the Ginzburg-Landau free energy density of an immiscible Cahn-Hilliard fluid, where $g(\phi)$ is a double-well function $g(\phi) = (1/4)(1-\phi^2)^2$. The logarithmic term in $\mathcal{F}_{\psi}$ is the ideal part of the entropy of mixing, while the term $-w(c/2)\psi^2$ represents the energy associated with the lateral interaction between adjacent surfactant layers [17]. $\mathcal{F}_1$ is a general linear coupling between the liquid-liquid interface and the surfactant field, emerging from the regularization of the surface Dirac δ function [20]. Finally, $\mathcal{F}_{\mathrm{ex}}$ accounts for the extra energy due to the presence of the surfactant in the bulk phases [17]. Contrary to the work of Engblom *et al.* [20], we do not consider a coupling term $\propto\psi[\phi(1-\phi)]$ in $\mathcal{F}_1$, since it is equivalent to $\propto\psi\phi^2$ in $\mathcal{F}_{\mathrm{ex}}$. Note that the only asymmetric term of the free energy functional is $-we\phi\psi$, being responsible for different equilibrium mole fractions of the surfactant in the bulk phases.

The parameters w and κ are related to measurable microscopic quantities, such as the interfacial tension (σ_0) and interface width (δ_0), of the surfactant-free equilibrium liquid-liquid interface via

$$w = (3/2)\,(\sigma_0/\delta_0) \quad \text{and} \quad \kappa = (3/4)\,(\sigma_0\,\delta_0). \tag{2}$$

The interface width is defined by the planar interface solution of the CH model $\phi^*(x) = \tanh(x/\delta_0)$, while the interfacial tension is associated with the parameters via the integral $\sigma_0 = \int_{-\infty}^{+\infty} dx\{\mathcal{F}_{\mathrm{CH}}[\phi^*(x)]\}$. The parameters related to the presence of the surfactant are interpreted as follows: $w/\beta = (RT)/v_0$, where v_0 is the average molar volume of the system, R the gas constant, and T the temperature. The model parameter β^{-1} then reads

$$\beta^{-1} = \frac{2}{3}\frac{RT}{v_0}\frac{\delta_0}{\sigma_0}. \tag{3}$$

Furthermore, the model parameter a is responsible for the exclusion of the surfactant in the bulk phases, while λ_1 and λ_2 control the coupling of the surfactant at the liquid-liquid interface. Introducing the length scale

$$\lambda = \sqrt{\kappa/(2\,w)} = \delta_0/2$$

and the free energy scale $H = w\,\lambda^D$, where D is the spatial dimensionality of the problem, results in

$$\tilde{F} = \int d\tilde{V}\{\tilde{\mathcal{F}}_{\mathrm{CH}} + \tilde{\mathcal{F}}_{\psi} + \tilde{\mathcal{F}}_{1} + \tilde{\mathcal{F}}_{\mathrm{ex}}\}, \tag{4}$$

with

$$\tilde{\mathcal{F}}_{\rm CH} = g(\phi) + (\tilde{\nabla}\phi)^2,$$
$$\tilde{\mathcal{F}}_{\psi} = \beta^{-1}[\psi\log\psi + (1-\psi)\log(1-\psi)] - \frac{c}{2}\psi^2,$$
$$\tilde{\mathcal{F}}_{1} = -\psi[\lambda_1 g(\phi) + \lambda_2(\tilde{\nabla}\phi)^2],$$
$$\tilde{\mathcal{F}}_{\rm ex} = \psi\left(\frac{a}{2}\phi^2 - e\phi\right).$$

Note that the dimensionless surfactant-free interfacial tension and interface width became

$$\tilde{\sigma}_0 = 4/3 \quad \text{and} \quad \tilde{\delta}_0 = 2,$$

respectively.

B. Euler-Lagrange equations

The equilibrium solutions represent extrema of the free energy functional with respect to the variables and can be obtained from the Euler-Lagrange equations,

$$\frac{\delta\tilde{F}}{\delta\phi} = \tilde{\mu}_\phi \quad \text{and} \quad \frac{\delta\tilde{F}}{\delta\psi} = \tilde{\mu}_\psi, \tag{5}$$

where $\delta\tilde{F}/\delta\phi$ and $\delta\tilde{F}/\delta\psi$ denote the functional derivatives of $\tilde{F}$ with respect to ϕ and ψ, respectively:

$$\frac{\delta\tilde{F}}{\delta\phi} = (1-\lambda_1\psi)(\phi^3-\phi) + (a\phi - e)\psi - 2\tilde{\nabla}[(1-\lambda_2\psi)\tilde{\nabla}\phi], \tag{6}$$

$$\frac{\delta\tilde{F}}{\delta\psi} = \frac{1}{\beta}\log\left(\frac{\psi}{1-\psi}\right) - c\,\psi + \hat{f}[\phi]. \tag{7}$$

Here the operator $\hat{f}[\phi]$ reads

$$\hat{f}[\phi] = -[\lambda_1 g(\phi) + \lambda_2(\tilde{\nabla}\phi)^2] + \left(\frac{a}{2}\phi^2 - e\,\phi\right). \tag{8}$$

Furthermore, $\tilde{\mu}_\phi = (\delta\tilde{F}/\delta\phi)|_{\phi^-,\psi^-}$ and $\tilde{\mu}_\psi = (\delta\tilde{F}/\delta\psi)|_{\phi^-,\psi^-}$ are constant background potentials corresponding to the homogeneous background states $\phi(\mathbf{r}) \equiv \phi^-$ and $\psi(\mathbf{r}) \equiv \psi^-$. The planar equilibrium interface solution $\phi^*(\tilde{x})$, $\psi^*(\tilde{x})$ can be obtained by solving the one-dimensional (1D) Euler-Lagrange equations with the boundary conditions

$$\phi^*(\tilde{x}\to\pm\infty) \to \phi^\pm, \quad \psi^*(\tilde{x}\to\pm\infty) \to \psi^\pm,$$
$$[d\phi^*(\tilde{x})/d\tilde{x}]_{\tilde{x}\to\pm\infty} = [d\psi^*(\tilde{x})/d\tilde{x}]_{\tilde{x}\to\pm\infty} \to 0,$$

where $\phi^\pm$ and $\psi^\pm$ can be determined as a function of the surfactant load (ψ_0) from the equilibrium conditions (see Sec. III B).

C. Dynamic equations

The time evolution of the system is governed by a simple diffusion dynamics,

$$\tau_\phi\frac{\partial\phi}{\partial t} = \nabla^2\frac{\delta F}{\delta\phi},$$
$$\tau_\psi\frac{\partial\psi}{\partial t} = \nabla\cdot\left[\tilde{M}(\phi)\psi(1-\psi)\nabla\frac{\delta F}{\delta\psi}\right],$$

where the term $\psi(1-\psi)$ in the second equation is necessary to achieve a regular diffusional equation for ψ in the bulk phases, while $\tilde{M}(\phi) \in [0,1]$ prescribes the relative mobility of ψ in the different phases and across the interface. The relaxation times τ_ϕ and τ_ψ can be related to diffusion coefficients as follows: Taking the first equation for $\psi(\mathbf{t},t) \equiv 0$ yields $\partial_t\phi = D_\phi\nabla^2[(\phi^3-\phi) - (\kappa/w)\nabla^2\phi]$, where $D_\phi = w/\tau_\phi$ is the diffusion coefficient of the phase separating liquid. Note that this is just half of the real diffusion coefficient D_0, since we have to take the equation for $\phi = \pm1 + \delta\phi$, where $|\delta\phi| \ll 1$, yielding the real diffusion equation $\partial_t\delta\phi = D_0\nabla^2\delta\phi$ with $D_0 = 2D_\phi$. Besides, in a bulk phase ($\phi \equiv \pm1$) the second equation of motion results in $\partial_t\psi = D_\psi\nabla^2\psi$ (if $c\psi \ll \beta^{-1}\log[\psi/(1-\psi)]$), where $D_\psi = \beta^{-1}(w/\tau_\psi)$ is the diffusion constant of the surfactant. Introducing the time scale

$$\tau = \lambda^2\frac{\tau_\phi}{w} = \frac{\delta_0^2}{2D_0}$$

results in

$$\frac{\partial\phi}{\partial\tilde{t}} = \tilde{\nabla}^2\frac{\delta\tilde{F}}{\delta\phi}, \tag{9}$$

$$\tilde{\tau}_\psi\frac{\partial\psi}{\partial\tilde{t}} = \tilde{\nabla}\cdot\left[\tilde{M}(\phi)\psi(1-\psi)\tilde{\nabla}\frac{\delta\tilde{F}}{\delta\psi}\right], \tag{10}$$

where

$$\tilde{\tau}_\psi = \frac{\beta^{-1}}{2}\frac{D_0}{D_\psi}. \tag{11}$$

For the sake of simplicity, we do not use tildes hereafter.

III. ANALYSIS

First, we analyze the equilibrium properties of the model. We calculate the interfacial tension as a function of the surfactant load in the constant surfactant field approximation, i.e., when the spatial variation of the equilibrium emulsifier profile is neglected. We show how the critical point (i.e., where the interfacial tension vanishes) enters the model, determine the interface width and the dynamic factor (the speed of phase separation), and show how these quantities behave for different surfactant couplings. Next, we analyze the existence criterion of the surfactant-free solution and the adsorption isotherms as a function of the critical point. Finally, we give a precise analytical approximation for the interfacial tension in a variant of the model in which the surfactant load dependence of the interface width is canceled.

A. Constant surfactant field approximation

Following the method of Engblom *et al.* [20], first we study the model in the constant surfactant field approximation. The simplest case is when the model is symmetric (i.e., $e = 0$). Since in this case the equilibrium planar interface is represented by an odd function, $\mu_\phi = 0$ [20]. Therefore, one can write $\phi^\pm = \pm\phi_0$ and $\psi^\pm = \psi_0$. ϕ_0 can be determined as a function of ψ_0 from Eq. (6) by introducing $\phi := \phi_0\hat{\phi}$ so that ϕ_0 represents the bulk equilibrium value of ϕ. Setting $x \to \pm\infty$, where $\hat{\phi} = \pm1$, then yields

$$\phi_0^2 = \frac{1-(\lambda_1+a)\psi_0}{1-\lambda_1\psi_0}. \tag{12}$$

Note that Eq. (12) is *exact* for $e = 0$, and this suggests a *critical point*,

$$\psi_c = \frac{1}{\lambda_1 + a}, \tag{13}$$

at which ϕ_0 vanishes (as long as $a \neq 0$), i.e., no phase separation occurs. Since ψ_c is only the function of λ_1 and a, and does not depend on the particular form of F_ψ, the critical point exists in the models of Theissen and Gompper [12], van der Sman and van der Graaf [14], Liu and Zhang [17], Li and Kim [18], Engblom *et al.* [20], and Yun *et al.* [19]. Using Eq. (12) and taking $\psi(x) \equiv \psi_0$, Eq. (6) simply becomes the Euler-Lagrange equation of a CH model, $\hat{\phi}^3 - \hat{\phi} = 2\,\partial^2_{\hat{x}}\hat{\phi}$, with the *rescaled* length $x = \xi\,\hat{x}$, where

$$\xi^2 = \frac{1 - \lambda_2\,\psi_0}{1 - (\lambda_1 + a)\psi_0}, \tag{14}$$

and the planar interface solution can be approximated as

$$\phi^*(x) = \phi_0\,\tanh[x/(2\xi)]. \tag{15}$$

Similarly to the Euler-Lagrange equation, using the constant surfactant approximation in the dynamic equation described by Eq. (9) yields $\partial_{\hat{t}}\hat{\phi} = \hat{\nabla}^2[g'(\hat{\phi}) - 2\hat{\nabla}^2\hat{\phi}]$ with the rescaled time $t = \hat{t}/s$, where the *dynamic factor* (defined as the inverse of the time scale) reads

$$s = \frac{1 - (\lambda_1 + a)\psi_0}{\xi^2}. \tag{16}$$

The speed of the phase separation can be considered as $v = \frac{d(L/\xi)}{dt}$, where L is the characteristic wavelength of the pattern. Therefore, using the scales yields $v = s\hat{v}$; i.e., the speed of phase separation is proportional to s. In the constant surfactant field approximation the interfacial tension reads

$$\sigma = \int_{-\infty}^{+\infty} dx\{\mathcal{F}[\phi^*(x)] - \mathcal{F}_0\}, \tag{17}$$

where $\mathcal{F}[\phi^*(x)]$ is the integrand of Eq. (4) evaluated for Eq. (15) and $\psi^*(x) = \psi_0$, while $\mathcal{F}_0 = \mathcal{F}[\phi^*(x), \psi^*(x)]_{x\to-\infty}$. The relative interfacial tension then reads

$$\kappa := \frac{\sigma}{\sigma_0} = \xi\phi_0^2\,[1 - (\lambda_1 + a)\psi_0], \tag{18}$$

where $\sigma_0 = 4/3$ is the interfacial tension of the surfactant-free system. Note that Eqs. (16) and (18) report that both the phase separation speed and the interfacial tension vanish at the critical point. Figure 1 shows the relative interface width [$\xi = (1 - d\,\psi_0)^{y_\xi}$], the dynamic factor [$s = (1 - d\,\psi_0)^{y_s}$], and the relative interfacial tension [$\kappa = (1 - d\,\psi_0)^{y_\kappa}$] as a function of the surfactant load in the constant surfactant field approximation for different surfactant field couplings (see Table I) in the case of $\lambda_1 + \lambda_2 \gg a$ and for $\psi_c < 1$. In this case the surfactant load dependence of the interface width is significant: The original model using the regularization of the surface Dirac δ function $(\nabla\phi)^2$ results in unphysical behavior; namely, the interface width vanishes together with the divergence of the speed of phase separation. In contrast, the regularization proposing $g(\phi)$ gives a more physical result, since the speed of phase separation decreases with decreasing interfacial tension together with increasing interface width.

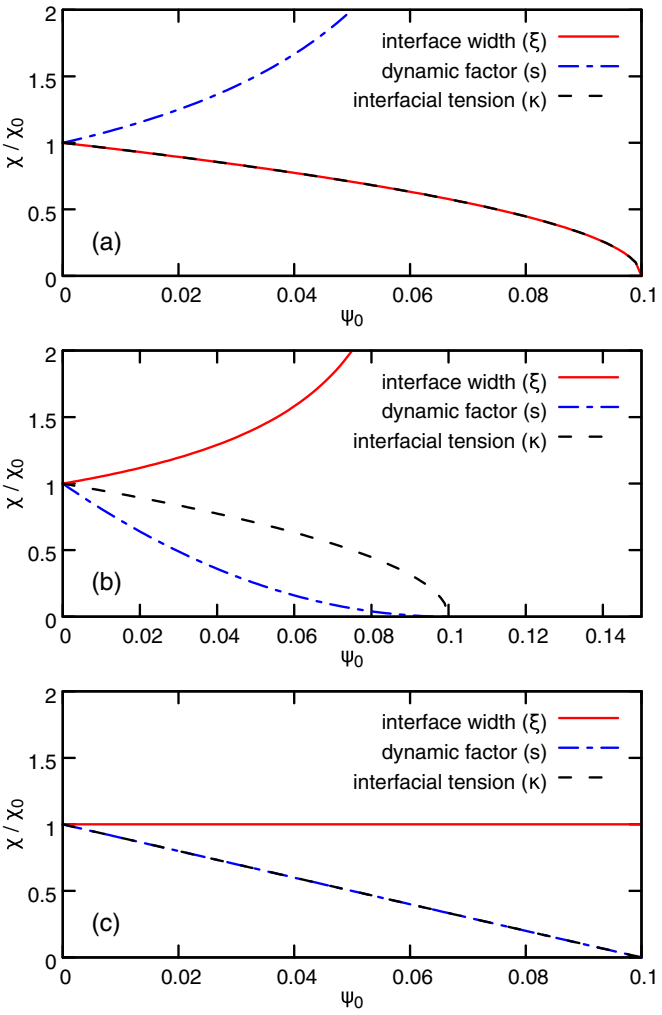

FIG. 1. (Color online) Relative interface width, phase separation speed (dynamic factor), and interfacial tension as a function of the surfactant load in the constant surfactant field approximation in the case of (a) the pure gradient ($\lambda_1 = 0$, $\lambda_2 = d$), (b) the fourth-order polynomial ($\lambda_1 = d$, $\lambda_2 = 0$), and (c) the proposed ($\lambda_1 = d$, $\lambda_2 = a + d$) surfactant field couplings. (See also Table I.)

Unfortunately, however, the critical point is practically inaccessible numerically, because of the divergent interface width: even an infinitesimal difference in the surfactant load can result in orders of magnitude change in the interface width. To resolve this problem, we propose a variant of the model where $\lambda_1 = d$ and $\lambda_2 = a + d$, yielding a constant interface width, independen of the model parameters a, d, c, and β.

TABLE I. Exponents of the relative interface width [$\xi = (1 - d\,\psi_0)^{y_\xi}$], dynamic factor [$s = (1 - d\,\psi_0)^{y_s}$], and relative interfacial tension [$\kappa = (1 - d\,\psi_0)^{y_\kappa}$] in the case of $\lambda_1, \lambda_2 \gg a$ and $\psi_c \leqslant 1$ for different surfactant couplings.

λ_1	λ_2	y_ξ	y_s	y_κ
0	d	1/2	−1	1/2
d	0	−1/2	2	1/2
d	$a + d$	0	1	1

Thus, the entire $\psi_0 = 0 \ldots \psi_c$ range becomes accessible in one single simulation, which becomes important when one wants to address the migration of the surfactant from loaded places to empty regimes, for example.

B. Adsorption isotherms

1. Existence of the $\psi \equiv 0$ solution

Considering Eq. (7) it is obvious that $\delta F/\delta\psi = \mu_\psi$ is an algebraic equation, yielding the 1D equilibrium profile $\psi^*(x)$ in the implicit form

$$\psi^*(x) = \frac{\psi^-}{\psi^- + (1-\psi^-)\exp\{\beta\,\Delta\hat{f}[\phi^*(x)] - c\,\Delta\psi^*(x)\}}, \tag{19}$$

where $\Delta\psi(x) = \psi^*(x) - \psi^-$ and

$$\Delta\hat{f}[\phi^*(x)] = \hat{f}[\phi^*(x)] - \hat{f}[\psi^-]. \tag{20}$$

Note that $\psi^*(x) \equiv 0$ is a solution of Eq. (19), since $\psi^- = \Delta\psi^*(x) = 0$, and $\beta\Delta f[\phi^*(x)]$ is bounded for $\phi^*(x) = \tanh(x/2)$. In contrast, this does not apply for models containing *no ideal mixing term* in F_ψ: In the model of Theissen and Gompper $\delta F/\delta\psi = s\psi - g_\psi\nabla^2\psi + \hat{f}[\phi]$ with $\hat{f}[\phi] = \gamma_1\phi^2 + \gamma_2 l^2(\nabla\phi)^2 + \gamma_3 l^4(\nabla^2\phi)^2$ [12], yielding the 1D Euler-Lagrange equation $\hat{f}[\phi^*(x)] = \hat{f}[\phi_b]$ for the surfactant-free solution $\phi^*(x) = \phi_b\tanh(x/\xi)$. Since $\gamma_{1,2,3}$ can be arbitrary, $f[\phi^*(x)] = \hat{f}[\phi_b]$ does not apply in general, therefore, the surfactant-free equilibrium planar interface is *not* a solution of the problem *in principle*. The derivation can be repeated in the case of the model of Li and Kim [18], yielding $d\phi^*(x)/dx = 0$ for the surfactant-free planar interface $\phi^*(x) = \tanh(x/\xi)$, which is definitely not true. These cases shed light on a general problem: The reduction of the free energy functional to the CH model is necessary but not sufficient for the surfactant-free planar interface to be the solution of the general model in the case of $\psi \equiv 0$. The reason for this is that first reducing the free energy, then solving the Euler-Lagrange equation(s) is identical to a conditional extremum problem, but a conditional extremum is not necessarily the extremum of the general problem at all. Finally, we mention that this discrepancy resulted in unrealistic adsorption isotherms in the aforementioned models, where the adsorbed amount of surfactant at the interface does not vanish even for zero far-field surfactant load.

2. Langmuir and Frumkin adsorption isotherms for $c = 0$

Besides ensuring the existence of the pure equilibrium planar interface solution, Eq. (19) plays one other important role: for $e = 0$ and $c = 0$ the adsorption isotherm reads

$$\psi_a(\psi_0) = \frac{\psi_0}{\psi_0 + (1-\psi_0)\exp[\beta\,\theta(\psi_0)]}, \tag{21}$$

where $\psi_a(\psi_0) = \psi^*(x)|_{x=0}$ is the surfactant mole fraction at the interface as a function of the bulk surfactant load ψ_0, and $\theta(\psi_0) = \Delta\hat{f}[\phi^*(x)]|_{x=0}$, namely,

$$\theta(\psi_0) = \left(\frac{\phi_0}{2\xi}\right)^2\left\{\xi^2\left[\lambda_1\left(\phi_0^2 - 2\right) - 2\,a\right] - \lambda_2\right\}. \tag{22}$$

Considering Eqs. (12) and (14) one can identify three *characteristic points* of the $\psi_a(\psi_0)$ curve: As long as $\theta(\psi_0)$ is bounded on $\psi_0 \in [0,1]$,

$$\psi_a(0) = 0 \quad \text{and} \quad \psi_a(1) = 1$$

apply. Moreover, since $\theta(\psi_c) = 0$, a third characteristic point also exists, namely,

$$\psi_a(\psi_c) = \psi_c.$$

Since the model has the *absolute* scale $\psi_0 \in [0,1]$, there are two essentially different cases:

(i) Previous works typically considered $\psi_c > 1$ [14,20], for which we have only the first two characteristic points together with $\psi_a(\psi_0) \in [0,1]$ on $\psi_0 \in [0,1]$. In this case, the Langmuir isotherms can be derived from Eq. (21) as follows: If $\theta(\psi_0) \approx \theta(0)$, and $\exp[\beta\theta(0)]$ is small enough to approximate the prefactor as $1 - \psi_0 \approx 1$, the well-known Langmuir adsorption isotherm

$$\psi_a \approx \frac{\psi_0}{\psi_0 + \Psi} \tag{23}$$

emerges with $\Psi = \exp[\beta\theta(0)]$. Converting the model parameters used by both van der Sman and van der Graaf [14] and Engblom *et al.* for Model 0 [20] results in $a = 1/2$, $\lambda_1 = 0$, $\lambda_2 = 1$, and $\beta \gtrsim 8$, respectively. Therefore, $\psi_c = 2$ was used in their work, while $\theta(0) = -1/2$ and $\exp[\beta\theta(0)] \lesssim 0.018$ was small enough to use Eq. (23) over almost the entire range $\psi_0 \in [0,1]$ [see Fig. 2(a)]. We note that Eq. (22) starts as

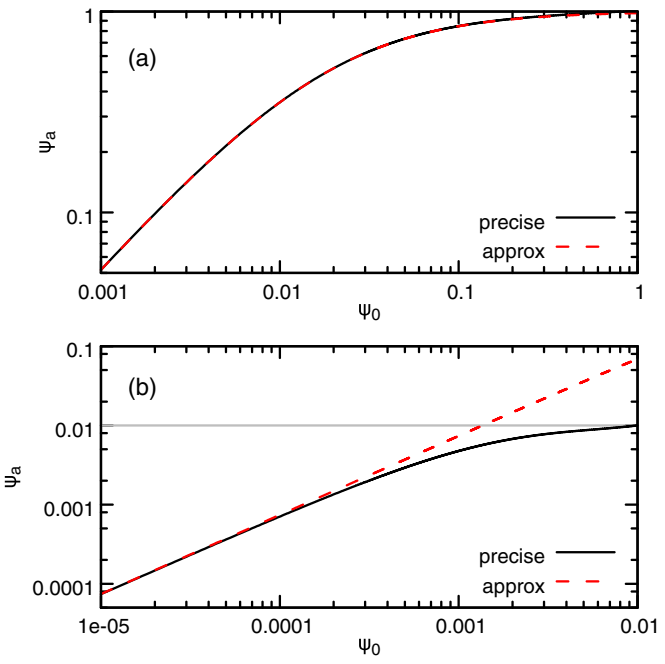

FIG. 2. (Color online) Adsorption isotherms from Eq. (21) (solid black line) and Eq. (23) [dashed (red) line] in the case of $\psi_c = 2$ (a) and $\psi_c = 0.01$ (b). The corresponding model parameters are $a = 1/2$, $\lambda_1 = 0$, $\lambda_2 = 1$, and $\beta = 8$ for (a) [14], and $a = 201$, $\lambda_1 = -101$, $\lambda_2 = 100$, and $\beta = 1/120$ for (b). Note the strong error of the Langmuir isotherm described by Eq. (23) in (b) for $\psi_0/\psi_c \gtrsim 0.1$.

$\theta(\psi_0) = -(1/2) + (1/8)\psi_0 + O(\psi_0^2)$, therefore we have

$$\psi_a(\psi_0) = \frac{\psi_0}{\psi_0 + \Psi \exp(\beta\,\theta_1\,\psi_0)} \tag{24}$$

in the first order, which becomes a Frumkin adsorption isotherm for lateral interaction parameters strong enough to win over $\theta_1\psi_0$, namely, $c(\psi_a - \psi_0) > \theta_1\psi_0$ [see Eq. (19)], as also suggested by Engblom *et al.* [20].

(ii) In the present work we focus on $\psi_c < 1$. Figure 2(b) shows the breakdown of the Langmuir adsorption isotherm for $\psi_0 \approx \psi_c$, indicating that Eq. (21) must be considered instead of Eq. (23). For the sake of interest, we mention that, although $\psi_a(\psi_0) \in [0,1]$ for $\psi_0 \in [0,1]$ still applies, $\psi_a(\psi_0) \in [0,\psi_c]$ does not necessarily apply for $\psi_0 \in [0,\psi_c]$. This means that it is possible to overload the interface for $\psi_0 \in (0,\psi_c)$ in principle, however, $\psi_a(\psi_c) = \psi_c$ is still valid. This can be seen in Fig. 5 of Engblom *et al.* [20]: For Model 2 the parameters read $a = 1$ and $\lambda_1 = \lambda_2 = 0$, yielding $\psi_c = 1$. For Model 3, $a = 1/2$, $\lambda_1 = 1$, and $\lambda_2 = 0$, indicating $\psi_c = 2/3$. The Langmuir isotherms give a reasonable estimation for the absorbed amount of surfactant at the interface for $\psi_0 < 0.1$, which is far from the critical value in both cases, and it is obvious that the interface load can be higher than $2/3$ in the case of Model 3.

Finally, we give the general condition of adsorption. The Taylor expansion of Eq. (21) [and also that of Eq. (23)] yields $\psi_a(\psi_0) = \exp[-\beta\theta(0)]\psi_0 + O(\psi_0^2) > \psi_0$, from which $\theta(0) < 0$ follows, indicating

$$2\,a + \lambda_1 + \lambda_2 > 0 \tag{25}$$

as the general condition for adsorption.

C. A more precise estimation for the interfacial tension

In order to understand the role of model parameters and apply the model for real systems, more sophisticated analytical calculation for the interfacial tension is needed. First, we approximate the equilibrium planar surfactant profile by taking into account the algebraic Euler-Lagrange equation, Eq. (7), instead of the constant field approximation. Then we present calculations for the interfacial tension in our proposed model $\lambda_1 = d$ and $\lambda_2 = a + d$ in both the symmetric ($e = 0$) and the general asymmetric ($e \neq 0$) case.

1. Symmetric case

As discussed above, now we take into account that the equilibrium planar surfactant profile $\psi^*(x)$ varies in space. Since Eq. (7) cannot be solved analytically for $c \neq 0$, first we assume that $\psi^*(x)$ remains *sufficiently close* to ψ_0 to use the second-order Taylor expansion of the logarithmic term in $\mathcal{F}_\psi$ around ψ_0. Then we expand Eq. (7) for $\phi^*(x)$ defined by Eq. (15) and $\psi^*(x) = \psi_0 + \delta\psi^*(x)$ with respect to $\delta\psi^*(x)$ up to the linear order, yielding

$$\delta\psi^*(x) \approx \frac{\Delta\hat{f}[\phi^*(x)]}{c - \frac{1}{\beta\,\psi_0\,(1-\psi_0)}}, \tag{26}$$

where $\Delta\hat{f}[\phi^*(x)]$ is defined by Eq. (20) with $\phi^- = -\phi_0$. Since there are two *leading terms* in $\Delta f[\phi^*(x)]$, namely, $g[\phi^*(x)] \propto \mathrm{sech}^4(x/2)$ and $[\partial_x\phi^*(x)]^2 \propto \mathrm{sech}^4(x/2)$, $\psi^*(x)$ is simply approximated as

$$\delta\psi^*(x) \approx A\,\mathrm{sech}^4(x/2), \tag{27}$$

where the amplitude A can be calculated by taking Eqs. (26) and (27) at $x = 0$, yielding

$$A = \frac{\theta(\psi_0)}{c - \frac{1}{\beta\,\psi_0\,(1-\psi_0)}}, \tag{28}$$

where $\theta(\psi_0)$ is defined by Eq. (22). In the symmetric case $\mu_\psi = 0$, therefore, the interfacial tension simply reads as

$$\sigma = \int_{-\infty}^{+\infty} dx\{\mathcal{F}[\phi^*(x),\psi^*(x)] - \mathcal{F}_0 - \mu_\psi[\psi^*(x) - \psi_0]\}.$$

Using Eqs. (15) and (27), and taking into account the Taylor expansion of the logarithmic term in $\mathcal{F}_\psi$ up to the second order, the interfacial tension reads

$$\sigma = \sigma_{\mathrm{CH}} + \sigma_\psi + \sigma_1 + \sigma_{\mathrm{ex}}, \tag{29}$$

where

$$\sigma_{\mathrm{CH}} = \sigma_0\big[\phi_0^2\big(2 - \phi_0^2\big)\big], \tag{30}$$

$$\sigma_\psi = \frac{32}{35}A^2\left[\frac{1}{\beta\,\psi_0(1-\psi_0)} - c\right], \tag{31}$$

$$\sigma_1 = -\frac{2}{105}\phi_0^2\big[8A\,\big(3\,a + 10\,d - 4\,d\,\phi_0^2\big) + 35\big(a + 4\,d - 2\,d\,\phi_0^2\big)\,\psi_0\big], \tag{32}$$

$$\sigma_{\mathrm{ex}} = -\frac{2}{15}a\,\phi_0^2(8\,A + 15\,\psi_0), \tag{33}$$

where ϕ_0 and A are defined by Eqs. (12) and (28), respectively. The first correction to the constant surfactant field approximation around $\psi_0 = 0$ comes from the Taylor expansion of Eq. (29),

$$\kappa = 1 - (2a + d + q)\psi_0 + O\big(\psi_0^2\big), \tag{34}$$

where $q = [(33a^2 + 40ad + 12\,d^2)/70]\beta$, accounting for the correction due to $\psi^*(x) \neq \psi_0$. Note that Eq. (18) reads $\kappa = 1 - (2a + d)\psi_0 + O(\psi_0^2)$ for $\lambda_1 = d$ and $\lambda_2 = a + d$; i.e., Eq. (34) starts with a different slope at $\psi_0 = 0$.

2. Asymmetric case

In the case of $e \neq 0$ Eq. (8) is not symmetric, yielding the general bulk equilibrium solution $\phi^+ \neq \phi^-$ and $\psi^- \neq \psi^+$. Therefore, one has to consider the full equilibrium problem,

$$\mu_\phi^+ = \mu_\phi^-, \tag{35}$$

$$\mu_\psi^+ = \mu_\psi^-, \tag{36}$$

$$\omega^+ = \omega^-, \tag{37}$$

where $\omega = \mathcal{F} - \mu_\phi^\pm\,\phi - \mu_\psi^\pm\,\psi$ is the grand potential density, whereas $\mu_\phi^\pm = \mu_\phi|_{\phi^\pm,\psi^\pm}$, $\mu_\psi^\pm = \mu_\psi|_{\phi^\pm,\psi^\pm}$, and $\omega^\pm = \omega|_{\phi^\pm,\psi^\pm}$. Note that there are four variables ($\phi^\pm$ and $\psi^\pm$) and three equations. Since we are interested in the physical quantities as a function of the surfactant load ψ_0, we introduce

$$\phi^\pm = \pm\phi_0 \pm \delta\phi_\pm \quad \text{and} \quad \psi^\pm = \psi_0 \pm \delta\psi_0, \tag{38}$$

where ϕ_0 is defined by Eq. (15) and ψ_0 is the only free parameter, the "average" surfactant load $\psi_0 = (\psi^- + \psi^+)/2$. (Note that this is not the real average, since the extra amount of the surfactant at the interface is not considered here.) This variable transformation is convenient, since the equilibrium values reduce to the symmetric solution for $e = 0$. Assuming that e and c are chosen so that $|\delta\psi_0/\psi_0|$ and $|\delta\phi_\pm/\phi_0|$ are sufficiently small, Eqs. (35)–(37) can be expanded *up to linear order* in $\delta\psi_0$ and $\delta\phi_\pm$ around the symmetric solution, resulting in

$$\delta\psi_0 = \frac{e\,\phi_0}{\mu_{\psi\psi} - \mu_{\phi\phi}^{-1}\left[e^2 + \left(\mu_{\phi\psi}^0\right)^2\right]}, \tag{39}$$

$$\delta\phi_\pm = \frac{e \mp \mu_{\phi\psi}^0}{\mu_{\phi\phi}}\,\delta\psi_0, \tag{40}$$

where $\mu_{\phi\phi} = (\partial^2\mathcal{F}/\partial\phi^2)|_{\phi_0,\psi_0}$, $\mu_{\psi\psi} = (\partial^2\mathcal{F}/\partial\psi^2)|_{\phi_0,\psi_0}$, and $\mu_{\phi\psi}^0 = (\partial^2\mathcal{F}/\partial\phi\partial\psi)|_{\phi_0,\psi_0}^{e=0}$. The equilibrium planar interfaces can be written as

$$\phi_a^*(x) \approx \phi^*(x) + \delta\phi_a^*(x),$$
$$\psi_a^*(x) \approx \psi^*(x) + \delta\psi_a^*(x),$$

where the corrections are defined as

$$\delta\phi_a^*(x) = \delta\phi_+\,\frac{\tanh\left(\frac{x}{2}\right)+1}{2} + \delta\phi_-\,\frac{\tanh\left(\frac{x}{2}\right)-1}{2}, \tag{41}$$

$$\delta\psi_a^*(x) = \delta\psi_0\,\tanh\left(\frac{x}{2}\right) + (B - A)\,\mathrm{sech}^4(x/2) \tag{42}$$

(see Fig. 3). Here B is determined at $x = 0$, where $\phi_a^*(0) = (\phi^- + \phi^+)/2$ and $\psi_a^*(0) = \psi_0 + B$. Expanding the Euler-Lagrange equation described by Eq. (7) up to first order around ψ_0 results in

$$B = \frac{\Delta\hat{f}[\phi_a^*(x)]_{x=0}}{c - \frac{1}{\beta\psi_0(1-\psi_0)}} - \delta\psi_0, \tag{43}$$

which reduces to Eq. (28) for $e = 0$. When calculating the interfacial tension, one has to take into account that Eqs. (35)–(37) have been taken up to first order in calculating

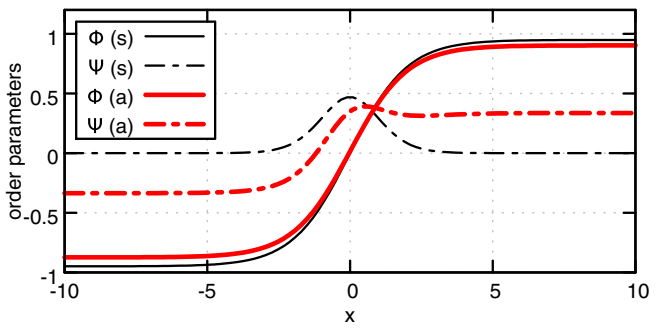

FIG. 3. (Color online) Equilibrium planar interfaces as predicted by Eqs. (15) and (27) in the symmetric case ($e = 0$; solid and dashed black curves) case and with the corrections described by Eqs. (41) and (42) for the asymmetric case [$e = 8$; solid and dashed (red) curves], respectively, with the parameters $\beta^{-1} = 100$, $d = 10$, $a = 1$, and $\psi_0 = 0.05$. Surfactant interfaces are normalized as $\Psi(x) = \beta^{-1}[\psi^*(x) - \psi_0]$.

equilibrium, the correction to the interfacial tension must be calculated accordingly. The interfacial tension is calculated as

$$\sigma = \int_{-\infty}^{+\infty} dx\{\omega - \omega^-\}, \tag{44}$$

where the thermodynamic grand potential density has been expanded in Eq. (37) around the symmetric solution $\phi^*(x)$ and $\psi^*(x)$ up to linear order as

$$\omega \approx \mathcal{F}^{(1)} - \mu_\phi^\pm\,\phi^*(x) - \mu_\psi^\pm\,\psi^*(x) - \mu_{\phi,0}^\pm\,\delta\phi^*(x) - \mu_{\psi,0}^\pm\,\delta\psi^*(x), \tag{45}$$

where $\mu_\phi^\pm$ and $\mu_\psi^\pm$ are taken up to first order in $\delta\phi^\pm$ and $\delta\psi^\pm$ around the symmetric solutions $\mu_{\phi,0}^\pm$ and $\mu_{\psi,0}^\pm$, respectively [the same applies for $\mathcal{F}^{(1)}$; i.e. it is taken around $\mathcal{F}_0$ up to first order with respect to $\delta\phi_a^*(x)$, $\delta\psi_a^*(x)$, and their spatial derivatives]. Note that although the terms containing $\mu_{\phi,0}^\pm$ and $\mu_{\psi,0}^\pm$ cancel in the bulk phases, $\mu_{\psi,0}^- \neq \mu_{\psi,0}^+$ and $\mu_{\phi,0}^- \neq \mu_{\phi,0}^+$ in general, because of the presence of the asymmetric term. Therefore, Eq. (45) is not *univalent* at the interface. Apparently this was the price of using the linear approximation for both the background potentials and the grand potential density. To resolve this discrepancy, we introduce the "average" grand potential density instead of Eq. (45) as

$$\bar{\omega} := \mathcal{F}^{(1)} - \bar{\mu}_\phi\,\phi^*(x) - \bar{\mu}_\psi\,\psi^*(x) - \bar{\mu}_{\phi,0}\,\delta\phi^*(x) - \bar{\mu}_{\psi,0}\,\delta\psi^*(x), \tag{46}$$

where $\bar{\mu}_\phi = (\mu_\phi^+ + \mu_\phi^-)/2$ and $\bar{\mu}_\psi = (\mu_\psi^+ + \mu_\psi^-)/2$. Note that Eq. (46) is univalent and $\bar{\mu}_\psi^+ = \bar{\mu}_\psi^-$, and it is also easy to show that it results in the equilibrium condition identical to Eq. (37), i.e., $\omega^+ = \omega^- \Leftrightarrow \bar{\omega}^+ = \bar{\omega}^-$. After some trivial algebraic manipulation and integration the interfacial tension reads

$$\sigma = \sigma_{e=0} + \sigma_{\delta g} + \sigma_\psi + \sigma_{\delta\phi} + \sigma_{\delta\psi}, \tag{47}$$

where $\sigma_{e=0}$ is the interfacial tension in the symmetric case defined by Eq. (29), while the corrections read

$$\sigma_{\delta g} = \frac{4\,\phi_0}{105}\{12(A - B)(a + d)\phi_0 - \Delta\phi_+[24\,A\,(a + d) - 35\,(1 - \{a + d\}\psi_0)]\},$$
$$\sigma_\psi = -2\,e\,\delta\psi_0(\mu_{\phi\psi}^0/\mu_{\phi\phi}),$$
$$\sigma_{\delta\phi} = \frac{4}{105}\phi_0\,\Delta\phi_+\{7[15 - 2\,a\,A + 2\,A\,d + 15(a - d)\psi_0] - 2\,\phi_0^2(70 + 3\,A\,d - 70\,d\,\psi_0)\} + \frac{8}{3}Ae\Delta\phi_-,$$
$$\sigma_{\delta\psi} = \frac{192\,A(A - B)}{105\,\beta\,\psi_0(\psi_0 - 1)} + \frac{4}{105}\{48\,A(A - B)c + \phi_0[105\,e\,\delta\psi_0 + 4(A - B)\phi_0(7\{a + d\} - 4\,d\,\phi_0^2)]\},$$

where $\Delta\phi_\pm = [(\delta\phi_-) \pm (\delta\phi_+)]/2$. It is trivial that $A - B \propto e$, meaning that the correction terms are proportional to e; i.e., they all vanish for $e \to 0$. The relative interface tension reads

$$\kappa = 1 - (2\,a + d + q)\psi_0 + \left(p + \frac{2\,a^3\beta^2}{35}e\right)\psi_0^2 + O\left(\psi_0^3, e^2\right), \tag{48}$$

where $p = a^2 + (\beta/70)\{66a^3 + 8ad(5 + d - 5c\beta) - 12d^2(c\beta - 1) + 3a^2[11(1 - c\beta) + 18d]\}$ and q is defined after Eq. (34). Therefore, the asymmetry has only a marginal effect on the interfacial tension near $\psi_0 = 0$, however, the behavior of the interfacial tension near the critical point necessitates further analysis.

D. Analysis near the critical point

While the interfacial tension and the interface width for the surfactant-free system are natural units of the theory, the critical point ψ_c is defined by exclusively the properties of the emulsifier via Eq. (13). Substituting $\psi_0 = \psi_c$ into Eqs. (29) and (47) also yields $\kappa = 0$ (for $a \neq 0$), therefore, the critical point is independent of the values of β, c, and e, showing the robustness of the theory. In the symmetric case the relative interfacial tension near the critical point can be obtained by expanding Eq. (29) around ψ_c for $\delta\bar{\psi} = \psi_0 - \psi_c \leqslant 0$, resulting in

$$\kappa = \left[\frac{33\,\alpha + 70\,a\,\psi_c^2\,(1 + c\,\psi_c\,\alpha)}{70\,a^2\,\psi_c^5\,(1 + c\,\psi_c\,\alpha)}\right]\delta\bar{\psi}^2 + O(\delta\bar{\psi}^3), \quad (49)$$

where $\alpha = \beta(\psi_c - 1)$. Comparing Eq. (49) to the results of previous work on the interfacial tension lowering [defined as $\Delta\sigma = (\kappa - 1)\sigma_0$] indicates that the previously suggested $\Delta\sigma \propto \log(1 - k\psi_0)$ relationship is not true for $\psi_0 \lesssim \psi_c \ll 1$. This is not surprising, taking into account that $\Delta\sigma \propto \log(1 - k\psi_0)$ emerges from the Langmuir isotherm described by Eq. (23). Accordingly, in the work of van der Sman and van der Graaf [14] the logarithmic expression has been found valid even for $\psi_0 = 0 \ldots 0.7$, due to the fact that $\psi_c = 2$ applied in that case, and the Langmuir isotherm was valid over almost the entire range $\psi_0 \in [0,1]$. In contrast, in the work by Liu and Zhang [17] the $\log(1 - k\,\psi_0)$ fit clearly shows a strong error at significant surfactant loads, where the Langmuir isotherm is not valid anymore (this is typical for $\psi_c \approx 1$).

Equation (49) plays an important role also from the viewpoint of spontaneous emulsification: If the coefficient of $\delta\bar{\psi}^2$ is non-negative, spontaneous emulsification cannot happen at $\psi_0 < \psi_c$, since the interfacial tension is non-negative over the entire range. In contrast, one can achieve negative interfacial tensions for $\psi_0 < \psi_c$ when

$$c > c_e = -\frac{33}{70\,a\,\psi_c^3} + \frac{\beta^{-1}}{\psi_c(1 - \psi_c)} \quad (50)$$

applies (or, in other words, when the interaction between adjacent surfactant layers is strong enough). In these cases an *emulsification* point ($\psi_e < \psi_c$) appears (see Fig. 4), at which the interfacial tension vanishes with finite ϕ_0. In addition, above ψ_e emulsification starts spontaneously due to hydrodynamic instabilities emerging from the negative interfacial tension.

It is important to mention that the analysis is not straightforward in the asymmetric case. Although both $\delta\phi_\pm \to 0$ and $\phi_0 \to 0$ apply for $\psi_0 \to \psi_c$, Eq. (40) results in $\delta\phi_\pm/\phi_0 = -1 + O(\sqrt{\delta\bar{\psi}})$ (where $\delta\bar{\psi} = \psi_c - \psi_0 \geqslant 0$), while $\delta\phi_\pm/\phi_0 \equiv 0$ for $e = 0$. This indicates a qualitatively different behavior of the interfacial tension near the critical point in the case of $e = 0$ and $e \neq 0$: Although the interfacial tension vanishes for $\psi_0 = \psi_c$ exactly for any $e \in \mathbb{R}$, Eq. (47) may not converge for $\psi_0 \to \psi_c$ in the case of $e \neq 0$. This discrepancy emerges from the linear approximation of Eqs. (35)–(37), however, a more accurate derivation is beyond the scope of the present work.

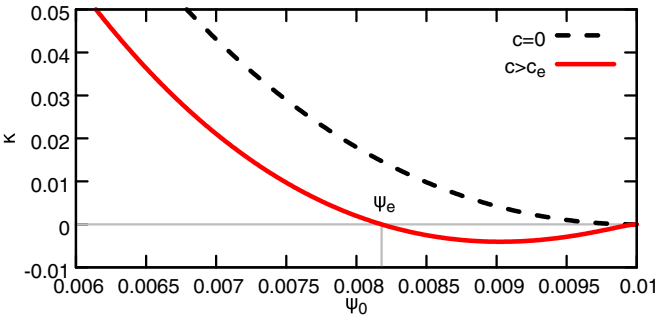

FIG. 4. (Color online) Relative interfacial tension κ as a function of the surfactant load ψ_0, as predicted by Eq. (29) for $\beta^{-1} = 120$, $a = 201$, and $d = -101$. Note that in the case of $c = 1.2 \times 10^4 > c_e = 9775.8$ an emulsification point, $\psi_e = 0.00818$, appears, above which spontaneous emulsification occurs due to the negative interfacial tension.

IV. NUMERICAL SIMULATIONS

A. Methodology

1. *Numerical solution of the Euler-Lagrange equations*

In order to validate Eq. (29), we determine the interfacial free energy using the numerical solution of the Euler-Lagrange equations described by Eqs. (6) and (7) as follows. Equation (6) is a second-order differential equation for ϕ, necessitating two boundary conditions to define a two-point boundary problem, while Eq. (7) is an algebraic equation prescribing the relationship between ϕ and ψ implicitly for a given ψ_0. The boundary conditions for the planar interface solution, however, read $\phi(x \to \pm\infty) \to \phi^\pm$, $\partial_x\phi(x \to \pm\infty) \to 0$, representing four constraints. Therefore, the problem is overdetermined, and in these cases shooting-type numerical integrators are not suitable in principle [22]. In addition, the problem is ill posed in the sense that it is translational invariant; namely, if $\phi^*(x)$ and $\psi^*(x)$ are a solution, then $\phi^*(x - x_0)$ and $\psi^*(x - x_0)$ are also a solution for any $x_0 \in \mathbb{R}$. Consequently, relaxation-type methods might also fail to converge on a finite range [22]. In order to avoid this problem, first we transform the equilibrium planar interface problem from an infinite-range problem into a finite-range problem by introducing the new independent coordinate:

$$\hat{x} := \tanh(x/2). \quad (51)$$

The new variables then read $\hat{\phi}(\hat{x}) = \{\phi[x(\hat{x})] - \Delta\}/h$, where $\Delta = -(\phi^- + \phi^+)/2$ and $h = (\phi^+ - \phi^-)/2$, yielding $\hat{\phi}(\pm 1) = \pm 1$, and $\hat{\psi}(\hat{x}) = \psi[x(\hat{x})]$. For the conversion, however, the values $\phi^\pm$ must be known, but these are known only for $e = 0$ analytically, therefore, we consider only the symmetric case hereafter, where $\hat{\phi}(\hat{x}) = \phi[x(\hat{x})]/\phi_0$. The spatial derivatives can be then expressed as

$$\partial_x\tilde{\phi} = t\,\partial_{\hat{x}}\hat{\phi}, \quad (52)$$

$$\partial_x^2\tilde{\phi} = t\left[t\left(\partial_{\hat{x}}^2\hat{\phi}\right) + \hat{x}(\partial_{\hat{x}}\hat{\phi})\right], \quad (53)$$

where $\tilde{\phi} = \phi/\phi_0$ and $t = 1/(\partial_{\hat{x}} x) = (1-\hat{x}^2)/2$. The Euler-Lagrange equations can be trivially transformed by using Eqs. (52) and (53) and solved with the boundary conditions $\hat{\phi}(\pm 1) = \pm 1$ and $\psi(\pm 1) = \psi_0$ using a relaxation method [22]. After having the solution $\hat{\phi}^*(\hat{x})$ and $\hat{\psi}^*(\hat{x})$ one can calculate the interfacial tension as

$$\sigma = \int_{-1}^{+1} d\hat{x}\{t\,(\mathcal{F}[\hat{\phi}^*(\hat{x}), \hat{\psi}^*(\hat{x})] - \mathcal{F}_0 - \tilde{\mu}_\psi[\hat{\psi}^*(\hat{x}) - \psi_0])\}, \quad (54)$$

where the integrand contains the transformed derivative $[\partial_x \phi^*(x)]^2 = [t\,\phi_0\,\partial_{\hat{x}}\hat{\phi}^*(\hat{x})]^2$, naturally.

2. Numerical solution of the dynamic equations

Equations (9) and (10) represent a fourth-order nonlinear parabolic PDE system. We use an advanced operator-splitting-based semi-implicit pseudospectral method developed by Tegze *et al.* [23] to solve the dynamic equations numerically with periodic boundary conditions. With this method the use of large time steps is allowed, contrary to the finite-difference method, where the stability criterion limits the time steps as h^4, where h is the spatial discretization step.

B. Parameters

For validation of the model/numerical simulations we determine the model parameters for a *model* system mimicking water/CO_2/macromolecular surfactant systems. Thus, the interfacial tension is of the order of 50 mJ/m^2 [24], and the width of the interface loaded by macromolecules is of the order of $\delta_0 \approx 0.1\ \mu$m [25]. The molecular weight of macromolecular surfactants is typically of the order of 1000 g/mol, while the density is considered to be approximately 1 g/cm^3 [26,27], yielding the average density of the system $\rho \approx 1000$ kg/m^3. We choose the critical point $\psi_c \approx 0.01$ [27], therefore, the average molar volume of the system can be approximated as $v_0 = 50\,\text{cm}^3/\text{mol}$. The liquid-liquid diffusion coefficient is typically $D_0 = 5 \times 10^{-9}$ m^2/s [28], and for the sake of simplicity, $\tilde{M}(\phi) = 1$ is chosen. The typical diffusion coefficient of macromolecules in water reads $D_\psi \approx 5 \times 10^{-11}$ m^2/s at room temperature ($T \approx 300$ K) [29]. Considering these physical parameters yields the model parameters

$$\beta^{-1} = 120 \quad \text{and} \quad \tilde{\tau}_\psi = 3600.$$

Furthermore, we choose

$$a = 201, \quad d = -101, \quad \text{and} \quad c = 0,$$

yielding a realistic κ curve with $\psi_c = 0.01$ [27]. Now one can see the huge difference between the cases considered previously and in this work by comparing Figs. 3 and 4 of Sagisaka *et al.* [27] to Fig. 3 of Liu and Zhang [17]. In the water/liquid CO_2/macromolecular surfactant system the interfacial tension drops suddenly for small surfactant loads ($\psi_0 \ll \psi_c \approx 0.01$), then it converges to 0 for $\psi_0 \to \psi_c$. In contrast, the relative interfacial tension lowering behaves qualitatively differently in the work by Liu and Zhang, prescribing slow changes for $\psi_0 \ll 1$ and fast changes for $\psi_0 \to 1$ (together with $\psi_c > 1$).

The Euler-Lagrange equations were solved for $e = 0$ as a function of the surfactant load to test the validity of our approximations for the interfacial tension, while the time evolution of the system was studied as a function of the surfactant load in two dimensions on a 1024×1024 grid with $\Delta x = \Delta y = \Delta t = 1$. The initial conditions were $\phi(\mathbf{r},0) = \phi_0(\Phi + \alpha\,\mathcal{R}[-1,1])$ and $\psi(\mathbf{r},0) = \psi_0$, where $\Phi \in [-1:1]$ is a fixed volume fraction, $\mathcal{R}[-1,1]$ is a random noise of uniform distribution on $[-1,1]$, and $\alpha \ll 1$.

C. Results

1. Interfacial tension

First, the validity of our analytic approximations for the interfacial tension is examined. Figure 5 shows the relative interfacial tension obtained from different approaches in the

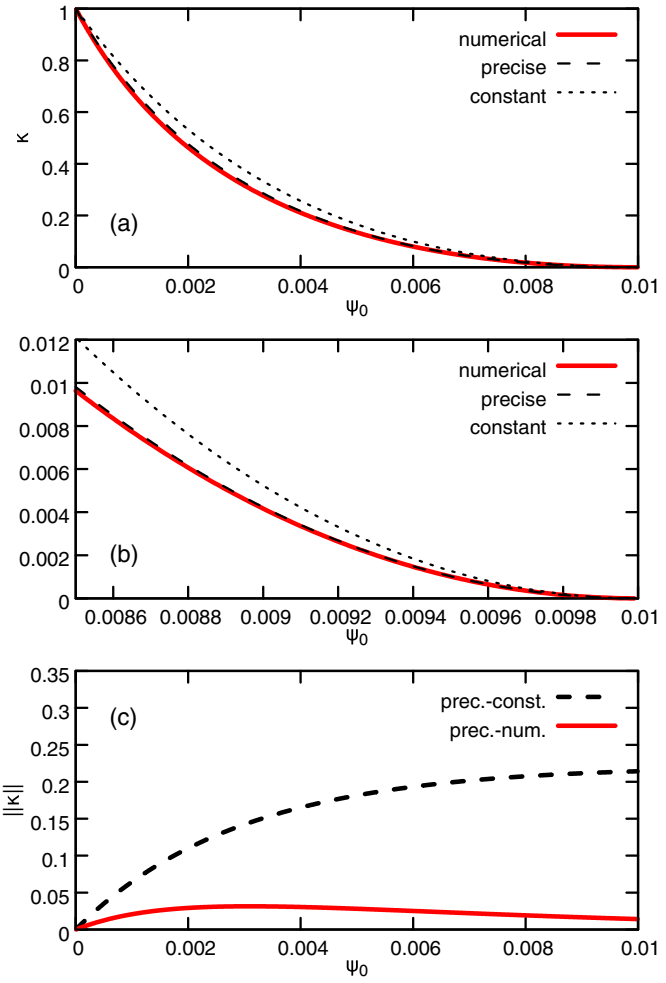

FIG. 5. (Color online) (a) Dynamic factor and relative interfacial tension predicted by different approaches (numerical solution of the Euler-Lagrange equations, precise analytical calculation, and constant surfactant field approximation) as a function of the surfactant load. (b) Magnification of (a) near the critical point $\psi_c = 0.01$. (c) Relative deviation $||\kappa|| = 2|(\sigma_1 - \sigma_2)/(\sigma_1 + \sigma_2)|$, where σ_1 and σ_2 are the interfacial tensions from the precise calculation and the constant surfactant approximation (dashed curve) and from the precise calculation and the numerical solution of the Euler-Lagrange equations (solid curve), respectively.

case of $e = 0$. Although the constant surfactant field approximation gives a reasonable estimation, Eq. (29) matches the numerical results almost perfectly. Since all curves converge to 0 in the case of $\psi_0 \to \psi_c$, it is worthwhile investigating the relative errors too. Both the constant surfactant approximation (compared to the more precise analytic approximation) and the analytic calculation (compared to the numerical results) show a finite relative error at the critical point, which means that $\sigma = a(\psi_c - \psi_0)^2 + O[(\psi_c - \psi_0)^3]$ applies for all curves, but with different a coefficients. We also note that the relative error between the precise analytic approximation and the numeric results shows a maximum at $\psi_0 \approx 0.0002$, which is due to the fact that the error increases with increasing deviation of the surfactant profiles obtained with the different methods. Since the surfactant profile is exactly 0 at $\psi_0 = 0$, and the interfacial tension vanishes at $\psi_0 = \psi_c$ (the solution is analytic in both cases), the interfacial tensions coincide at these points, regardless of the method we choose. Consequently, $|\sigma_1 - \sigma_2| = 0$ applies at $\psi_0 = 0$ and $\psi_0 = \psi_c$, but otherwise the error is finite in between, showing a maximum at $\psi_0 \in (0, \psi_c)$. The relative error slightly modifies this picture, since it can be finite at the critical point, for the reasons described above. Summarizing, the relative errors indicate that the model parameters should be fitted via Eq. (49) near the critical point rather than using Eq. (18), because the coefficient for the precise analytic estimation containing additional factors compared to (49) is in qualitatively better agreement with the numerical results. The importance of Eq. (29) is then twofold: First, the model can be calibrated for real systems *analytically*. Second, it shows that the critical point does not change as a function of the level of precision in determining the interfacial tension, showing the robustness of the theory.

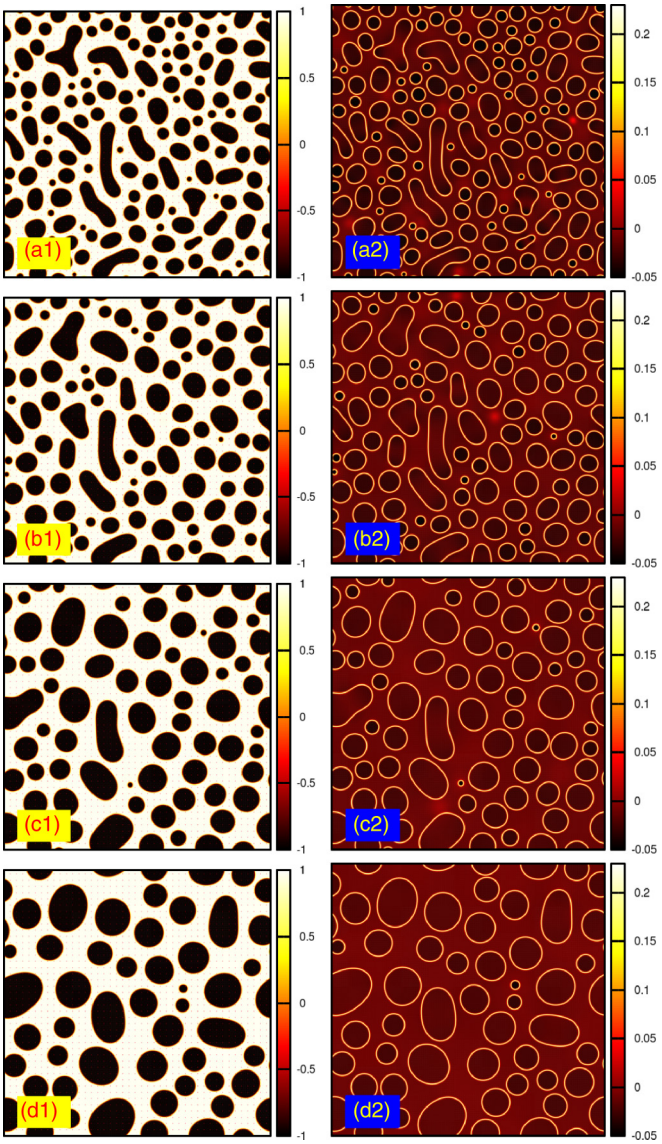

FIG. 6. (Color online) Time evolution of the system for average surfactant load $\psi_0 = 0.005$ in the case of $e = 0$. $\phi(\mathbf{r},t)/\phi_0$ and $[\psi(\mathbf{r},t)/\psi_0] - 1$ are shown in (a1)–(d1) and (a2)–(d2), respectively, at $t = 100$, 200, 500, and 1000 (time passes from top to bottom).

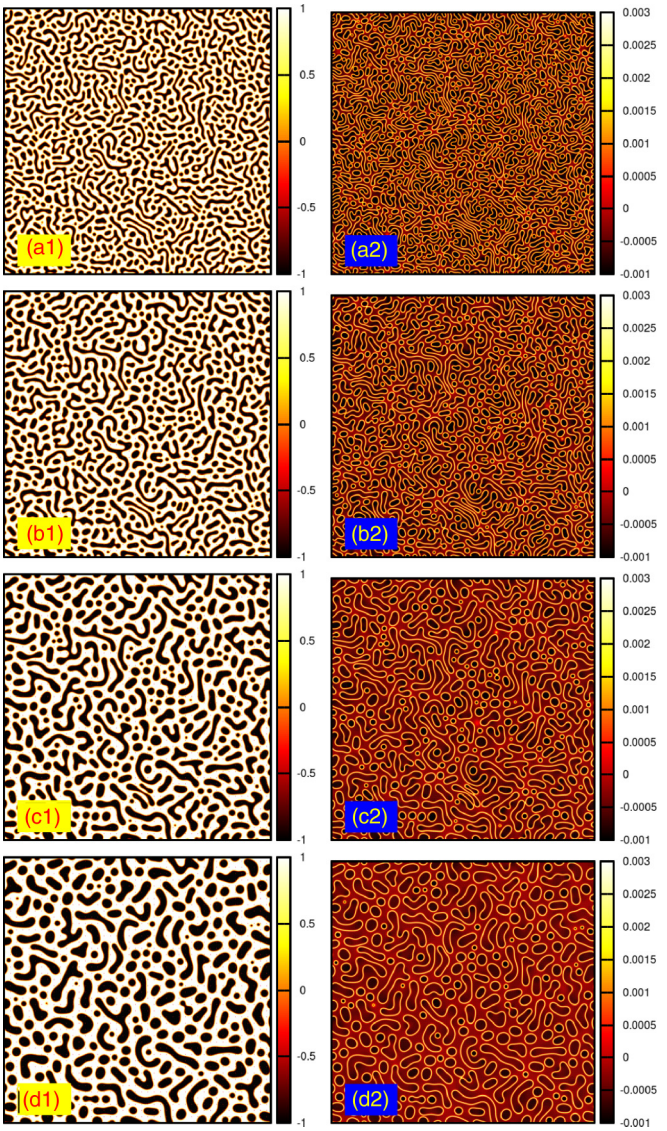

FIG. 7. (Color online) Time evolution of the system for average surfactant load $\psi_0 = 0.0099$ in the case of $e = 0$. $\phi(\mathbf{r},t)/\phi_0$ and $[\psi(\mathbf{r},t)/\psi_0] - 1$ are shown in (a1)–(d1) and (a2)–(d2), respectively, at $t = 100$, 200, 500, and 1000 (time passes from top to bottom).

2. *Phase separation*

(a) Symmetric case. The time evolution of the system was scanned as a function of ψ_0. Figures 6 and 7 show snapshots of the simulations at $t = 100, 200, 500$, and 1000 [corresponding to Figs. 6(a)–6(d) and 7(a)–7(d)] in the case of $\psi_0 = 0.005$ and $\psi_0 = 0.0099$, respectively. It can clearly be seen that the phase separation is significantly slower for $\psi_0 = 0.0099$ (Fig. 7) than for $\psi_0 = 0.005$ (Fig. 6). To quantify the results, we introduce the amount of liquid-liquid interfaces,

$$Q(t) := \int dV\{[\nabla\hat{\phi}(\mathbf{r},t)]^2\}, \tag{55}$$

where $\hat{\phi}(\mathbf{r},t) = \phi(\mathbf{r},t)/\phi_0 \in [-1,1]$ is the normalized liquid-liquid order parameter. Figure 8(a) shows $Q(t)$ for different surfactant loads ($\psi_0/\psi_c = 0.0, 0.25, 0.5, 0.75, 0.95, 0.99$, and 0.999 from bottom to top, respectively). The curves are linear and parallel to each other in the log-log plot, implying the *master curve*

$$Q(t) = [t/\tau(\psi_0)]^q, \tag{56}$$

where the time scale reads $\tau(\psi_0) = \exp[p(\psi_0)/q]$, while $p(\psi_0)$ and q are the parameters of the linear fit $\log[Q(t)] = p(\psi_0) - q\log(t)$. Equation (56) means that the qualitative behavior of the system is independent of the surfactant load, therefore, the dynamic factor can be written as

$$s = \frac{\tau(0)}{\tau(\psi_0)} = \exp[-\Delta p(\psi_0)/q], \tag{57}$$

where $\Delta p(\psi_0) = p(\psi_0) - p(0)$, i.e., the vertical distance between the lines corresponding to ψ_0 and $\psi_0 = 0$ in Fig. 8(a). The numerical simulations resulted in $q \approx 0.28$, while the distances read $\Delta p(\psi_0) = 0.0$, 0.228 22, 0.452 37, 0.708 46, 1.080 54, 1.509 33, and 2.169 71 (from bottom to top, respectively). The calculated dynamic factors are shown in Fig. 8(b), as a function of the surfactant load. It is obvious that the numerical dynamic factor (i.e., the relative speed of phase separation) follows the reduction of the interfacial tension, rather than Eq. (16), or, in other words, the dynamical system is driven by the interfacial tension. This is an important result, showing that even though the constant surfactant

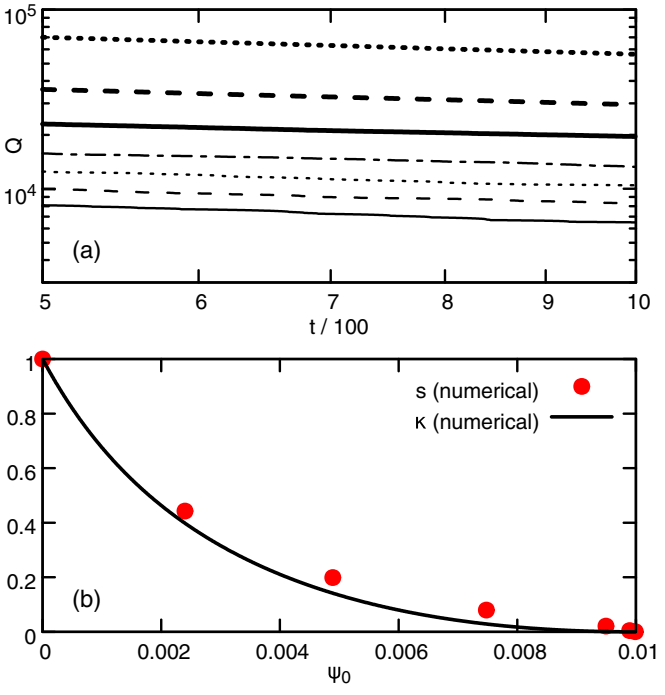

FIG. 8. (Color online) Time evolution of the symmetric system. (a) Amount of liquid-liquid interfaces as a function of time for average surfactant loads $\psi_0/\psi_c = 0.0, 0.25, 0.5, 0.75, 0.95, 0.99$, and 0.999 (from bottom to top). (b) Dynamic factor (or relative speed of phase separation) defined by Eq. (57) [(red) circles] at surfactant loads corresponding to those in (a), compared to the relative interfacial tension κ obtained from numerical solution of the Euler-Lagrange equations.

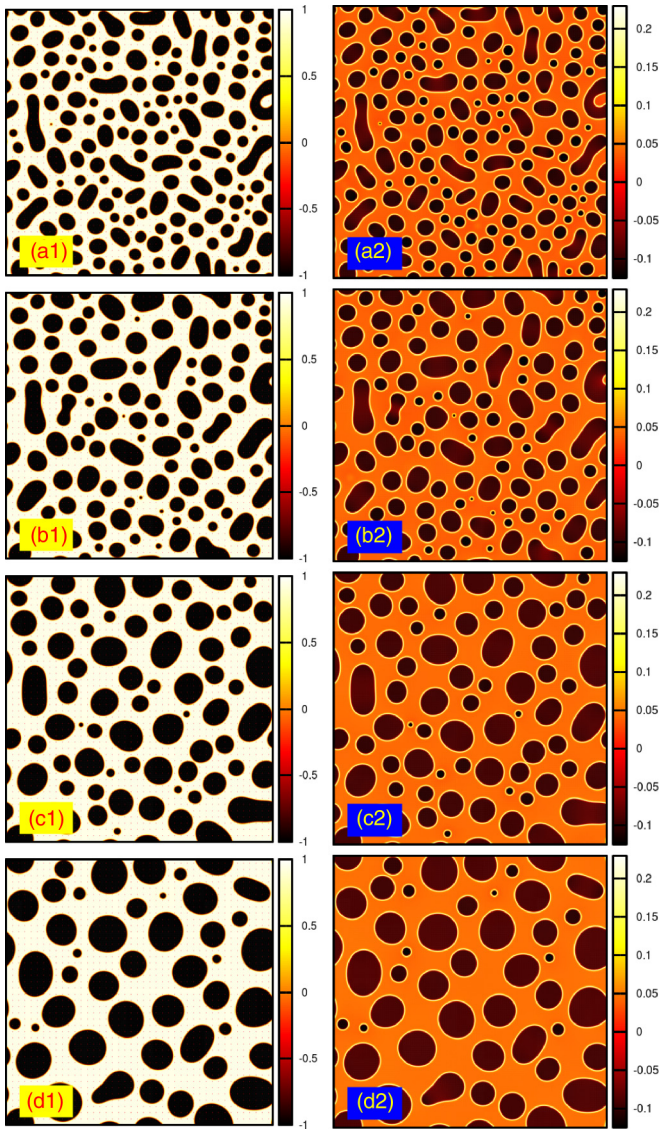

FIG. 9. (Color online) Time evolution of the asymmetric system for average surfactant load $\psi_0 = 0.005$. $\phi(\mathbf{r},t)/\phi_0$ and $[\psi(\mathbf{r},t)/\psi_0] - 1$ are shown in (a1)–(d1) and (a2)–(d2), respectively, at $t = 100$, 200, 500, and 1000 (time passes from top to bottom).

approximation results in a reliable estimation for the relative interfacial tension, it is absolutely not sufficient to predict the speed of phase separation. The error of s relative to κ is due to (i) finite-size effects and (ii) the fact that the surfactant load in the bulk phases changes constantly even during a single simulation because of the conservative dynamics (however, this change is less than 1% in our simulations).

(b) Asymmetric case. Finally, the effect of the asymmetry is investigated. We apply $e = 10$, yielding the estimated relative difference $|\delta\psi_0/\psi_0| \leqslant 10\%$, indicating significant asymmetry, as also shown in Figs. 9 and 10. Note, however, that Fig. 10 corresponds to $\psi_0 = 0.0097$ now, indicating a slight shift in the critical point due to the asymmetry. Furthermore, the amplitude of the surfactant at the interface vanishes relative to $\delta\psi_0$ near the critical point. Parallel to Fig. 8, Fig. 11 shows the numerical dynamic factor as a function of the surfactant load in the asymmetric case. The amount of liquid-liquid interfaces is defined again by Eq. (55), but with $\hat{\phi}(\mathbf{r},t) := 2\frac{\phi(\mathbf{r},t)-\phi^-}{\phi^+-\phi^-} - 1$, transforming the bulk values ϕ^- and ϕ^+ to -1 and $+1$, respectively (ϕ^+ and ϕ^- were measured from the simulations here). According to Fig. 11(b) it is clear that the asymmetry has only a marginal effect on the speed of phase separation compared to the symmetric case, which is in agreement with Eq. (48), showing that e is not of the leading order of κ. In addition, the marginal effect of the asymmetry applies over the entire range $\psi_0 \in [0, \psi_c^{e=10}]$, where the critical point is only slightly shifted compared to the symmetric system; namely, $\psi_c^{e=10} \approx 0.0098$ has been found (we had equal dynamical factors $s = 4 \times 10^{-4}$ for $\psi_0 = 0.00999$ and $\psi_0 = 0.0098$ in the case of $e = 0$ and $e = 10$, respectively). Summarizing, it has been shown that asymmetry plays only a secondary role in the model, even near the critical point, which is only slightly shifted for moderate asymmetry. Finally, we mention that in the case of asymmetry the transient times found are significantly smaller; i.e., pattern formation starts faster than in the case of $e = 0$. This is the reason why the time range $t = 10 \ldots 100$ has been chosen for measuring the dynamic factor, instead of $t = 500 \ldots 1000$, as in the case of $e = 0$. (Practically we chose ranges in which the $\log[Q(t)]$-vs-$\log(t)$ lines were parallel to each other, to make the measurement of s possible.) In this case the exponent $q = 0.26$ emerges with $\Delta p = 0.0$, 0.242 88, 0.459 53, 0.711 55, 1.068 20, 1.395 20, and 2.033 70, for the same average surfactant loads ψ_0/ψ_c used in the symmetric case, respectively.

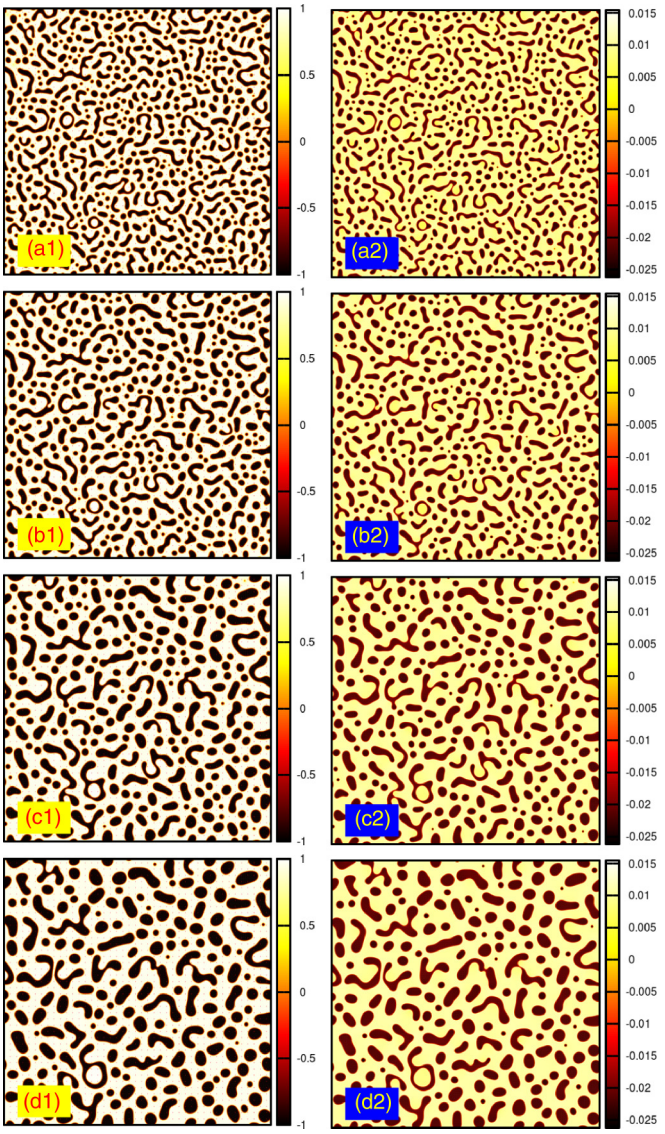

FIG. 10. (Color online) Time evolution of the asymmetric system for average surfactant load $\psi_0 = 0.0097$. $2\frac{\phi(\mathbf{r},t)-\phi^-}{\phi^+-\phi^-} - 1$ and $[\psi(\mathbf{r},t)/\psi_0] - 1$ are shown on (a1)–(d1) and (a2)–(d2), respectively, at $t = 100$, 200, 500, and 1000 (time passes from top to bottom).

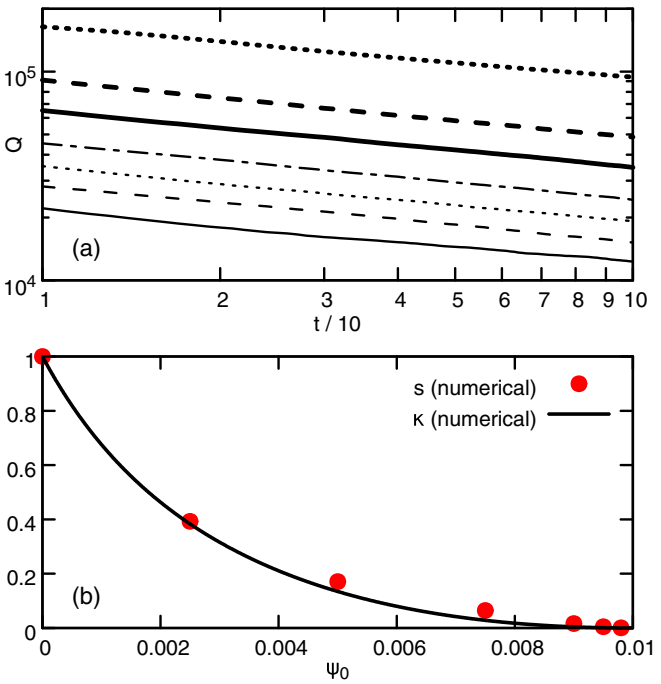

FIG. 11. (Color online) Time evolution of the asymmetric system. (a) Amount of liquid-liquid interfaces as a function of time for different average surfactant loads. (b) Dynamic factor (or relative speed of phase separation) defined by Eq. (57) [(red) circles] at surfactant loads corresponding to those in (a), compared to the relative interfacial tension κ obtained from numerical solution of the Euler-Lagrange equations in the case of $e = 0$.

V. CONCLUSIONS

In this work we have analyzed the Ginzburg-Landau free-energy-functional-based generalized van der Sman/van der Graaf–type diffuse interface model of surfactant-assisted phase separation. We have shown that different regularization of the surface Dirac δ function leads to different qualitative behavior in the speed of phase separation, equilibrium interfacial tension, and interface width as a function of the surfactant load. The original, gradient-square regularization yields unphysical behavior of both the interface width and the speed of phase separation. In contrast, using the double-well function instead yields a coherent physical picture, however, with a divergent interface width at the critical point ψ_c being present in the general model (the critical point ψ_c is the surfactant load where the interfacial tension vanishes). Accordingly, we proposed a hybrid regularization of the surface Dirac δ function, resulting in a constant interface width but a decreasing interfacial tension and phase separation speed as well, making the model numerically wieldy even near the critical point. Contrary to previous work, we analyzed the general model over the *entire* relevant surfactant load range, which reads $\psi_0 \in [0,1]$ for $\psi_c > 1$ and $\psi_0 \in [0,\psi_c]$ for $\psi_c \leqslant 1$, respectively. First, we have shown that a realistic Langmuir/Frumkin isotherm emerges from the presence of the logarithmic therm, which then must be used in physically consistent models. Second, since the amount of surfactant absorbed at the interface (i.e., the interface load) is equal to the bulk value (far-field load) at $\psi_0 = \psi_c$, it has been proven that the approximations made in previous work for the Langmuir/Frumkin isotherms are valid only for $\psi_c > 1$; however, the systems of interest may show even $\psi_c \ll 1$. In these cases, extended analysis is needed to investigate the qualitative behavior of the system when $\psi_0 \lesssim \psi_c$. The analysis was based on a precise analytical derivation of the interfacial tension, which was then validated by numerical calculations in the case of model parameters mimicking a real water/liquid CO_2/macromolecular surfactant system. The numerical results are in excellent agreement with the analytical calculations. Time-dependent simulations have also been performed, showing that (i) the qualitative behavior of the system is not a function of the surfactant load, and (ii) the speed of phase separation follows the reduction in the relative interfacial tension. It has also been shown that asymmetry (when bulk phases affect the presence of the surfactant field differently) enters the system only at second order around $\psi_0 = 0$ and it has only a minor effect on both the location of the critical point and the speed of phase separation as a function of the surfactant load. Finally, we mention that the interfacial tension has been found to vanish as $\propto(\psi_0 - \psi_c)^2$ near the critical point. In contrast, experiments clearly indicate $\propto \log(\psi_0/\psi_c)$ behavior over almost the entire range $\psi_0 \in [0,\psi_c]$ [27], yielding a linear relationship near ψ_c instead of a quadratic one, suggesting that spontaneous emulsification is possible in these systems. Such a situation can be described either by changing the model parameters appropriately to establish an emulsification point $\psi_e < \psi_c$, at which the interfacial tension vanishes, or by applying *nonlinear* coupling of the surfactant field at the level of the free energy functional. Moreover, since macromolecular surfactants result in a typical liquid-liquid interface width of the order of 0.1 μm, fluid flow may also play a significant role in the time evolution of the system. One must not forget that the dynamical equations used in this study describe diffusion-controlled processes but avoid the fast phase separation kinetics observed experimentally during liquid-liquid spinodal decomposition in binary systems. In other words, the liquid described by a pure diffusion-type equation cannot flow, so it must then be corrected appropriately. Nevertheless, there are different ways to introduce such a correction. The phenomenological approach is to modify Fick's law to describe the relaxing solute flux (finite speed of sound) instead of the instantaneous one, thus introducing a second time derivative for the chemical concentration accounting for a wave mode [30,31]. Another possibility is to simply apply the Navier-Stokes equation with an appropriate Korteweg pressure tensor, a problem which has been studied for binary [32,33] and multicomponent [34,35] systems, as well as for the case of surfactant-assisted liquid phase separation as mentioned earlier. Such a development, however, is a topic for future study.

ACKNOWLEDGMENTS

We thank Professor S. Engblom (Uppsala University, Sweden) for valuable discussions. This work was supported by VISTA basic research program Project No. 6359 ("Surfactants for water/CO_2/hydrocarbon emulsions for combined CO_2 storage and utilization") of the Norwegian Academy of Science and Letters and Statoil.

[1] J. Sjoblom, *Emulsions and Emulsion Stability: Surfactant Science Series 61* (Taylor & Francis, London, 1996).
[2] A. E. Hargreaves, in *Chemical Formulation* (RSC Paperbacks, Royal Society of Chemistry, London, 2003), pp. X001–X004.
[3] D. Halpern, O. E. Jensen, and J. B. Grotberg, J. Appl. Physiol. **85**, 333 (1998).
[4] B. A. Hills, J. Appl. Physiol. **87**, 1567 (1999).
[5] D. Sarker, *Pharmaceutical Emulsions: A Drug Developer's Toolbag* (Wiley, New York, 2013).
[6] D. Myers, *Surfactant Science and Technology* (Wiley, New York, 2005).
[7] G. Ahearn, J. Am. Oil Chem. Soc. **46**, 540A (1969).
[8] S. Iglauer, Y. Wu, P. Shuler, Y. Tang, and W. A. Goddard III, J. Petrol. Sci. Eng. **71**, 23 (2010).
[9] S. Q. Tunio, A. H. Tunio, N. A. Ghirano, and Z. M. El Adawy, Int. J. Appl. Sci. Tech. **1**, 143 (2011).
[10] Z. Song, Z. Li, M. Wei, F. Lai, and B. Bai, Comput. Fluids **99**, 93 (2014).
[11] G. Gompper and S. Zschocke, Phys. Rev. A **46**, 4836 (1992).
[12] O. Theissen and G. Gompper, Eur. Phys. J. B Condens. Matter Complex Syst. **11**, 91 (1999).
[13] T. Teramoto and F. Yonezawa, J. Colloid Interface Sci. **235**, 329 (2001).
[14] R. van der Sman and S. van der Graaf, Rheol. Acta **46**, 3 (2006).

[15] H. Diamant and D. Andelman, Europhys. Lett. **34**, 575 (1996).
[16] C.-H. Teng, I.-L. Chern, and M.-C. Lai, Discrete Cont. Dynam. Syst. B **17**, 1289 (2012).
[17] H. Liu and Y. Zhang, J. Comput. Phys. **229**, 9166 (2010).
[18] Y. Li and J. Kim, Eur. Phys. J. B **85**, 340 (2012).
[19] A. Yun, Y. Li, and J. Kim, Appl. Math. Comput. **229**, 422 (2014).
[20] S. Engblom, M. Do-Quang, G. Amberg, and A.-K. Tornberg, Commun. Comput. Phys. **14**, 879 (2013).
[21] K. E. Teigen, P. Song, J. Lowengrub, and A. Voigt, J. Comput. Phys. **230**, 375 (2011).
[22] W. H. Press, S. A. Teukolsky, W. T. Vetterling, and B. P. Flannery, *Numerical Recipes in C* (Cambridge University Press, Cambridge, 2002).
[23] G. Tegze, G. Bansel, G. I. Tóth, T. Pusztai, Z. Fan, and L. Gránásy, J. Comput. Phys. **228**, 1612 (2009).
[24] L. C. Nielsen, I. C. Bourg, and G. Sposito, Geochim. Cosmochim. Acta **81**, 28 (2012).
[25] E. Torino, E. Reverchon, and K. P. Johnston, J. Colloid Interface Sci. **348**, 469 (2010).
[26] S. S. Adkins, X. Chen, I. Chan, E. Torino, Q. P. Nguyen, A. W. Sanders, and K. P. Johnston, Langmuir **26**, 5335 (2010).
[27] M. Sagisaka, T. Fujii, Y. Ozaki, S. Yoda, Y. Takebayashi, Y. Kondo, N. Yoshino, H. Sakai, M. Abe, and K. Otake, Langmuir **20**, 2560 (2004).
[28] W. Lu, H. Guo, I. Chou, R. Burruss, and L. Li, Geochim. Cosmochim. Acta **115**, 183 (2013).
[29] M. G. Davidson and W. M. Deen, Macromolecules **21**, 3474 (1988).
[30] P. Galenko and D. Jou, Phys. Rev. E **71**, 046125 (2005).
[31] P. Galenko and V. Lebedev, Phys. Lett. A **372**, 985 (2008).
[32] G. Tegze, T. Pusztai, and L. Gránásy, Mater. Sci. Eng. A **413–414**, 418 (2005).
[33] G. Tegze and G. I. Tóth, Acta Mater. **60**, 1689 (2012).
[34] J. Kim and J. Lowengrub, Int. Free Bound. **7**, 435 (2005).
[35] J. Kim, Commun. Comput. Phys. **12**, 613 (2012).